



High energy ion acceleration by extreme laser radiation pressure

Paul McKenna
UNIVERSITY OF STRATHCLYDE VIZ ROYAL COLLEGE OF SCIENCE & TECHNOLOGY

03/14/2017
Final Report

DISTRIBUTION A: Distribution approved for public release.

Air Force Research Laboratory
AF Office Of Scientific Research (AFOSR)/ IOE
Arlington, Virginia 22203
Air Force Materiel Command

REPORT DOCUMENTATION PAGE				Form Approved OMB No. 0704-0188	
<p>The public reporting burden for this collection of information is estimated to average 1 hour per response, including the time for reviewing instructions, searching existing data sources, gathering and maintaining the data needed, and completing and reviewing the collection of information. Send comments regarding this burden estimate or any other aspect of this collection of information, including suggestions for reducing the burden, to Department of Defense, Executive Services, Directorate (0704-0188). Respondents should be aware that notwithstanding any other provision of law, no person shall be subject to any penalty for failing to comply with a collection of information if it does not display a currently valid OMB control number.</p> <p>PLEASE DO NOT RETURN YOUR FORM TO THE ABOVE ORGANIZATION.</p>					
1. REPORT DATE (DD-MM-YYYY) 14-03-2017		2. REPORT TYPE Final		3. DATES COVERED (From - To) 01 May 2013 to 31 Dec 2016	
4. TITLE AND SUBTITLE High energy ion acceleration by extreme laser radiation pressure				5a. CONTRACT NUMBER	
				5b. GRANT NUMBER FA8655-13-1-3008	
				5c. PROGRAM ELEMENT NUMBER 61102F	
6. AUTHOR(S) Paul McKenna				5d. PROJECT NUMBER	
				5e. TASK NUMBER	
				5f. WORK UNIT NUMBER	
7. PERFORMING ORGANIZATION NAME(S) AND ADDRESS(ES) UNIVERSITY OF STRATHCLYDE VIZ ROYAL COLLEGE OF SCIENCE & TECHNOLOGY 16 RICHMOND STREET GLASGOW, G1 1XT GB				8. PERFORMING ORGANIZATION REPORT NUMBER	
9. SPONSORING/MONITORING AGENCY NAME(S) AND ADDRESS(ES) EOARD Unit 4515 APO AE 09421-4515				10. SPONSOR/MONITOR'S ACRONYM(S) AFRL/AFOSR IOE	
				11. SPONSOR/MONITOR'S REPORT NUMBER(S) AFRL-AFOSR-UK-TR-2017-0015	
12. DISTRIBUTION/AVAILABILITY STATEMENT A DISTRIBUTION UNLIMITED: PB Public Release					
13. SUPPLEMENTARY NOTES					
14. ABSTRACT <p>A number of scientific breakthroughs were achieved on the topic of high power laser-driven ion acceleration and underpinning physics over the three-year duration of the grant. The most notable of these were published in high impact papers in Nature group journals and the leading physics journal, Physical Review Letters. Amongst the highlights is the experimental and numerical demonstration that during the interaction of an ultraintense laser pulse with an ultrathin foil target, a relativistic plasma aperture is produced, which can be used to control of the collective plasma electron motion via diffraction of the laser light. While this can reduce the effectiveness of the radiation pressure mechanism responsible for ion acceleration, it can also lead to additional acceleration mechanisms and optical control of the resultant ion beams. This work has been published in the leading international physics journal Nature Physics, and a related paper on the resulting influence of this relativistic plasma aperture on the accelerated ion dynamics has been published in Nature Communications. These results build on an earlier paper arising from the project investigating elliptical and lobe-like electron beam structures from ultrathin targets, published in New Journal of Physics. An additional follow-up paper with more detailed analysis of the electron behavior occurring from this aperture was also published in High Power Laser Science and Engineering.</p> <p>A significant breakthrough was also made, at an early stage in the grant, on the effects of lattice-melt-induced resistivity gradients on the transport of mega-ampere currents of fast electrons in solids. These fast electrons are responsible for forming the strong electrostatic fields which accelerate the ions. This work was published in the internationally leading journal Physical Review Letters. We continued to progress this pioneer</p>					
15. SUBJECT TERMS ion therapy, heavy ion acceleration, ultraintense lasers, radiation pressure, EOARD					
16. SECURITY CLASSIFICATION OF:			17. LIMITATION OF ABSTRACT	18. NUMBER OF PAGES 15	19a. NAME OF RESPONSIBLE PERSON CUMMINGS, RUSSELL
a. REPORT Unclassified	b. ABSTRACT Unclassified	c. THIS PAGE Unclassified			19b. TELEPHONE NUMBER (Include area code) 011-44-1895-616021

**HIGH ENERGY ION ACCELERATION BY EXTREME LASER RADIATION
PRESSURE**

GRANT: FA8655-13-1-3008

**Principle Investigator:
Paul McKenna**

**Period of Performance:
01-03-2014 to 01-03-2017**

TABLE OF CONTENTS

1. Summary

2. Introduction

3. Methods, assumptions and procedures

3.1 Experimental methods

3.1.1 Laser systems

3.1.2 Targets

3.1.3 Diagnostics

3.2 Numerical methods

3.2.1 EPOCH

3.2.2 Zephyros

4. Results and Discussion

4.1 Fast electron transport effects

4.2 Ion acceleration from ultrathin targets

4.3 Ion and electron structures induced by diffraction

5. Conclusions

6. Publications

7. References

LIST OF FIGURES

Figure 1 – An example of a Vulcan Petawatt experimental setup

Figure 2 – Electron structures induced via laser diffraction

Figure 3 – Ion structures formed from radiation pressure and sheath acceleration mechanisms

Figure 4 – 3D hybrid simulation results showing fast electron density maps

Figure 5 – Resistive instability growth rate

Figure 6 – 3D simulation results showing electron jet formation and influence

Figure 7 – 2D simulation density maps demonstrating electron jet directionality

Figure 8 – Intra-pulse dynamics of low-energy annular proton structures

1. SUMMARY

A number of scientific breakthroughs were achieved on the topic of high power laser-driven ion acceleration and underpinning physics over the three-year duration of the grant. The most notable of these were published in high impact papers in *Nature* group journals and the leading physics journal, *Physical Review Letters*. Amongst the highlights is the experimental and numerical demonstration that during the interaction of an ultraintense laser pulse with an ultrathin foil target, a 'relativistic plasma aperture' is produced, which can be used to control of the collective plasma electron motion via diffraction of the laser light. Whilst this can reduce the effectiveness of the radiation pressure mechanism responsible for ion acceleration, it can also lead to additional acceleration mechanisms and optical control of the resultant ion beams. This work has been published in the leading international physics journal *Nature Physics* [1], and a related paper on the resulting influence of this 'relativistic plasma aperture' on the accelerated ion dynamics has been published in *Nature Communications* [2]. These results build on an earlier paper arising from the project investigating elliptical and lobe-like electron beam structures from ultrathin targets, published in *New Journal of Physics* [3]. An additional follow-up paper with more detailed analysis of the electron behaviour occurring from this aperture was also published in *High Power Laser Science and Engineering* [4].

A significant breakthrough was also made, at an early stage in the grant, on the effects of lattice-melt-induced resistivity gradients on the transport of mega-ampere currents of fast electrons in solids. These fast electrons are responsible for forming the strong electrostatic fields which accelerate the ions. This work was published in the internationally leading journal *Physical Review Letters* [5]. We continued to progress this pioneering work and the role that it can play in laser-driven ion acceleration throughout the grant. This led to the publication of three additional papers on fast-electron transport physics in *Plasma Physics and Controlled Fusion* [6-8] and a paper investigating plasma density gradients for conversion to fast-electrons, published in *New Journal of Physics* [9].

Another notable breakthrough is our discovery that in ultrathin foils undergoing relativistic transparency, a plasma jet is formed which couples energy into the expanding ion population, giving rise to additional energy transfer to sheath-accelerated ions. This work was published in *New Journal of Physics* [10]. This investigation was continued to address the impact of the angular incidence of the laser pulse on the target and was published in *Nuclear Instruments and Methods A* [11]. For similar targets, it was found that by monitoring the divergence of a low-energy annular component in the accelerated ion beam, it is possible to observe the intra-pulse transition from sheath acceleration, through radiation pressure acceleration to transparency. This was published in *Physics of Plasmas* [12]. Through one-dimensional modelling of the interaction, it was also discovered that if populations of ions can be accelerated via RPA into the sheath accelerated population, energy exchange can occur via the ion-ion acoustic instability, and this is published in *Plasma Physics and Controlled Fusion* [13].

Overall this grant has been extremely successful at advancing the understanding of laser-plasma interactions, in particular relativistic induced transparency and its effects on multiple ion acceleration mechanisms. The results from this work will impact heavily on future developments of compact laser-driven ion sources and will help bring this technology to maturity.

2. INTRODUCTION

Ultra-intense laser ($>10^{18} \text{ Wcm}^{-2}$) interactions with solid matter can induce strong electrostatic fields that can accelerate ions to multi-MeV energies over micron-scale distances. By harnessing this behaviour it may be possible to develop compact ion acceleration devices for use in medical (oncology, radiotherapy), science (probing and radiography), industry and security (imaging) applications. It is therefore of vital importance to investigate the underlying physics of these interactions in order to bring this emerging laser-driven ion sources technology to maturity.

A variety of ion acceleration mechanisms exist and depend upon the laser pulse parameters and target composition. For relatively thick, micron-scale foil targets, at current peak laser intensities ($\sim 10^{21} \text{ Wcm}^{-2}$), the dominant ion acceleration mechanism is driven by sheath electric fields at the rear of the target, that are induced by the escape of fast electrons generated during the interaction of the laser pulse with the front surface of the target [14]. This process is termed target normal sheath acceleration (TNSA), as the ions are predominately accelerated in the target normal direction. As the target thickness is reduced to sub-micron levels, additional ion acceleration mechanisms begin to impact on the formation of the resulting ion beams. Direct action of the laser radiation pressure on the electrons at the front surface of the target can drive the critical surface (at which the plasma frequency is equal to the laser frequency) forward [15]. This is known as radiation pressure acceleration (RPA) and has been predicted to result in ion beams with a narrow energy spectrum, low divergence and favourable energy scaling with laser intensity [16,17]. This RPA mechanism is sensitive to the formation of transverse instabilities, which can be detrimental to the resulting ion beam [18]. As the target thickness is reduced further, it is possible for the target to undergo relativistic induced transparency (RIT) [19]. This occurs due to a reduction in electron density due to target expansion and the heating of the electron population to relativistic levels. This reduces the target plasma frequency below that of the laser frequency, resulting in the propagation of the remainder of the laser pulse. This effect can reduce the effectiveness of the RPA mechanism, but it can result in volumetric heating of the target electrons, which can lead to additional coupling of energy into the ions via the breakout afterburner (BOA) scheme [20,21].

The work undertaken as part of this grant has focused on developing our understanding of these varied acceleration mechanisms and the interplay between them. In TNSA, the propagation of fast-electrons through the target can be of importance to the formation of the sheath fields on the rear surface. Therefore, in order to establish the impact of this propagation, work was undertaken during the grant period to investigate the effects of various aspects of the target lattice structure and resistivity on the propagation of the fast-electrons through different target materials. This can greatly influence the resulting spatial profile of the accelerated TNSA ion beam.

Similarly, by investigating the effects of the transition from RPA to RIT we have made significant breakthroughs in understanding the underlying ion acceleration dynamics. In particular, if a target becomes relativistically transparent to the laser pulse, the propagation of the laser pulse can drive a collimated electron jet through the expanded TNSA layer of ions, enhancing the energy in a localised region. We have performed a series of studies that demonstrate this behaviour, potential secondary effects and a technique to diagnose the transition experimentally.

As RIT occurs within a localised region of the laser focal spot (where the laser intensity is highest), we also show that diffraction of the propagating laser pulse through this local 'relativistic plasma aperture' can lead to drastic changes in the rear surface electrons and accelerated ions. This paves the way for control of the accelerated structures through purely optical means.

3. METHODS, ASSUMPTIONS, AND PROCEDURES

The experimental and simulation methods used in this work are discussed in the relevant sections below.

3.1 Experimental methods

3.1.1 Laser systems

Gemini: The Gemini Ti:sapphire laser at the Rutherford Appleton Laboratory was used to produce pulses of 800 nm wavelength, λ , light, with typical duration, $\tau = 40 \text{ fs}$ (full width at half maximum, FWHM), spot

size of 3 μm (FWHM) and energy ~ 2 J (on-target, i.e. the energy after plasma mirrors and transport optics). The laser pulse duration could be varied in the range 40–160 fs by adding group velocity dispersion to the pulse via an acousto-optic modulator. A double plasma mirror arrangement can enhance the intensity contrast to $\sim 10^{11}$ and $\sim 10^9$, at 1 ns and 10 ps, respectively, prior to the peak of the pulse. The pulse was focused using an f/2 parabolic mirror, to a calculated peak intensity of $\sim 7 \times 10^{20}$ Wcm^{-2} . A deformable mirror was employed prior to focusing to ensure a high quality focal spot. The laser light could be linearly, elliptically or circularly polarized.

Vulcan Petawatt: The 1.054 μm -wavelength Vulcan laser at the Rutherford Appleton Laboratory was used to investigate multiple aspects of laser-driven ion acceleration. It was configured to deliver either a single pulse with duration equal to (1.0 ± 0.2) ps (FWHM) or a main pulse with a (1.0 ± 0.2) ps lower intensity prepulse, with peaks separated by (1.5 ± 0.1) ps. The latter mode respectively corresponds to a change in the intensity profile of the rising edge of the main pulse. This was achieved by introducing a pre-pulse after the first stage of pre-amplification, and before the pulse stretcher, using a polarizer and polarizing beam splitter to control the energy. The total laser pulse energy (on-target) was (200 ± 15) J and is typically fixed. The focal spot FWHM diameter was 7.3 μm , giving a calculated peak intensity, of 2×10^{20} Wcm^{-2} (for the single pulse case). A single plasma mirror was typically used in the focusing beam to enhance the contrast. A secondary, lower intensity laser pulse of 10 ps to 5 ns could also be used to drive long-time scale expansion of the target or as a secondary drive for proton emission.

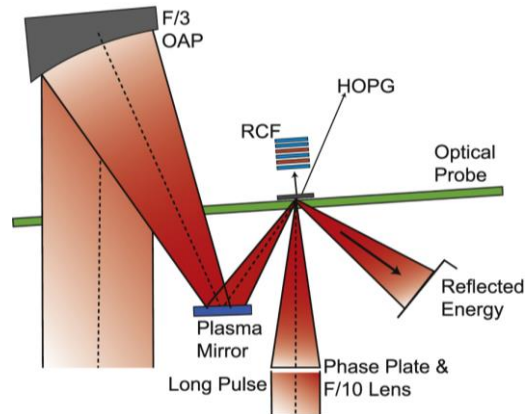


Figure 1. An example of a Vulcan Petawatt experimental setup

PHELIX: The PHELIX high power laser at GSI in Darmstadt was also used to generate S-polarised light with a central wavelength equal to 1.053 μm was delivered in pulses with duration (725 ± 100) fs and energy (180 ± 10) J. The beam was focused using an f/1.5 off-axis parabola into a 2.5 μm diameter (FWHM) spot, resulting in calculated peak intensity of $\sim 7 \times 10^{20}$ Wcm^{-2} .

3.1.2 Targets

A variety of solid density targets were used throughout the experiments. These consisted of aluminium, plastic, copper, silicon and gold targets with a range of thickness from 10nm-200 μm . Depending upon the physics investigated, these targets could be layered together or used as a separate proton source.

3.1.3 Diagnostics

Radiochromatic film stack: To detect and analyse the accelerated proton beams, a stack of radiochromatic film (RCF) was employed, with each film layer separated by an appropriate amount of shielding in order to detect both the spatial and energy profile of the protons. This was typically positioned a short distance (~ 6 cm) from the rear of the target. In some situations, a slot was cut through the centre of the stack in order to provide line of sight to additional diagnostics.

Image-plate: Layers of image-plate are positioned at the rear of the RCF stack in order to diagnose the accelerated electron beam profile.

Thomson parabola spectrometer: To separate and provide a measurement of the charge-to-mass ratio and energy spectrum of the different ion species accelerated, Thomson parabola spectrometers were typically employed using calibrated image plate. These could be positioned at various angles to the incoming laser pulse and the target normal to provide a sampling at the different angles of interest.

Optical probe: A transverse optical probe was aligned along the rear surface of the target in order to monitor plasma expansion in some experiments.

Highly Ordered Pyrolytic Graphite X-ray spectrometer: To diagnose changes to the laser energy coupling to fast electrons, $K\alpha$ emission from a buried Cu layer, the Cu- $K\alpha$ signal, which is produced by electrons

above 8.98 keV, were measured using two highly ordered pyrolytic graphite (HOPG) crystal spectrometers

3.2 Numerical methods

3.2.1 EPOCH Particle-in-Cell

The majority of numerical simulations were conducted using EPOCH, which is a fully relativistic, parallel, particle-in-cell (PIC) code that can be run in 1D, 2D or 3D. This code, given a set of initial parameters, solves Maxwell's equations using a finite-difference time-domain solver whilst moving a collection of macro-particles according to the Lorentz force. The resultant electric and magnetic fields from the macroparticles are fed back into the system and the code continues to iterate. In order to successfully resolve the necessary temporal and spatial structures, high-performance computing clusters were used (at the University of Strathclyde and using the UK national high performance computing resource), with individual simulations requiring up to ~50,000 core hours of resource, producing multiple terabytes of output data.

3.2.2 Zephyros hybrid PIC

Full collisional PIC simulations are very inefficient for thick (up to 200 μm) solid density targets. To account for this, the particle-based 3D-hybrid code Zephyros was used instead. This code makes the assumption that the background ion and electron behaviour can be approximated with a fluid model whilst simulating the electrons with particles similar to the PIC method.

4. RESULTS AND DISCUSSION

4.1 Ion and electron spatial structures induced by laser diffraction

Asymmetry in the collective dynamics of ponderomotively-driven electrons in the interaction of an ultraintense laser pulse with a relativistically transparent target was demonstrated, for the first time, experimentally. The 2D profile of the beam of accelerated electrons was shown to change from an ellipse aligned along the laser polarization direction in the case of limited transparency, to a double-lobe structure aligned perpendicular to it when a significant fraction of the laser pulse co-propagates with the electrons. The temporally-resolved dynamics of the interaction were also investigated via particle-in-cell simulations. The results provide new insight into the collective response of charged particles to intense laser fields over an extended interaction volume, which is important for a wide range of applications, and in particular for the development of promising new ultraintense laser-driven ion acceleration mechanisms involving ultrathin target foils. This work was published in *New Journal of Physics* [8].

With further investigation into this asymmetric effect, we showed that a 'relativistic plasma aperture' is generated in thin foils by intense laser light, resulting in the fundamental optical process of diffraction. The plasma electrons collectively respond to the resulting laser near-field diffraction pattern, producing a beam of energetic electrons with a spatial structure that can be controlled by variation of the laser pulse parameters, as can be seen in figure 1. It is shown that static electron-beam and induced-magnetic-field structures can be made to rotate at fixed or variable angular frequencies depending on the degree of ellipticity in the laser polarization. The concept was demonstrated numerically and verified experimentally, and is an important step towards optical control of charged particle dynamics in laser-driven dense plasma sources. This work was published in *Nature Physics* [11].

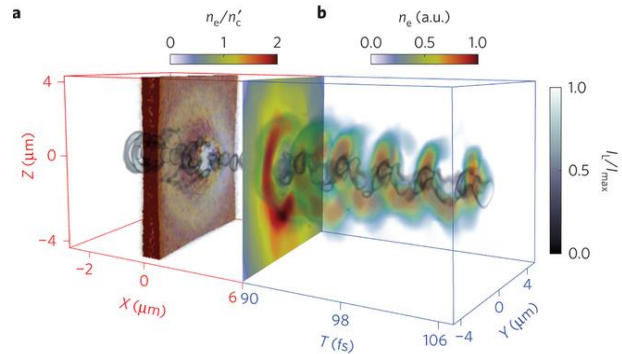


Figure 1. Combined plot showing the 3D laser intensity profile (up to $X = 6 \mu\text{m}$) at 100 fs (a); and the temporal evolution of the electron density distribution, overlaid with the laser intensity distribution (b), in the Y - Z plane at $X = 6 \mu\text{m}$ from 90 to 107 fs [11].

Additional studies of this phenomenon show that if the target is sufficiently thin that the laser induces significant radiation pressure, but not thin enough to become relativistically transparent to the laser light, the resulting relativistic electron beam is elliptical, with the major axis of the ellipse directed along the laser polarization axis. When the target thickness is decreased such that it becomes relativistically transparent early in the interaction with the laser pulse, we again show that diffraction of the transmitted laser light occurs through the 'relativistic plasma aperture', inducing structure in the spatial-intensity profile of the beam of energetic electrons. It was demonstrated that the electron beam profile can be modified by variation of the target thickness and degree of ellipticity in the laser polarization. This work was published in *High Power Laser Science and Engineering* [12].

Continuing the investigation into the impact of diffraction through this 'relativistic plasma aperture', we find the important result that shows that under these conditions, the electron dynamics are mapped into the beam of protons accelerated via strong charge-separation-induced electrostatic fields. It is demonstrated experimentally and numerically via 3D PIC simulations that the degree of ellipticity of the laser polarization strongly influences the spatial-intensity distribution of the beam of multi-MeV protons. The influence on both sheath-accelerated and radiation pressure-accelerated protons is investigated and example results shown in figure 2. This approach opens up a potential new route to control laser-driven ion sources and was published in *Nature Communications* [13].

4.2 Fast-electron transport effects

As there is typically always a degree of ion sheath acceleration, the impact of fast-electron transport effects were also studied. Numerical and experimental investigations into solid targets were performed to analyse the influence of lattice-melt-induced resistivity gradients on the transport of mega-ampere currents of fast electrons in solids using laser-accelerated protons to induce isochoric heating. Tailoring the heating profile enables the resistive magnetic fields which strongly influence the current propagation to be manipulated, as shown in figure 3. This tunable laser-driven process enables important fast electron beam properties, including the beam divergence, profile, and symmetry to be actively tailored, and without recourse to complex target manufacture. This work was published in the leading physics journal, *Physical Review Letters* [1].

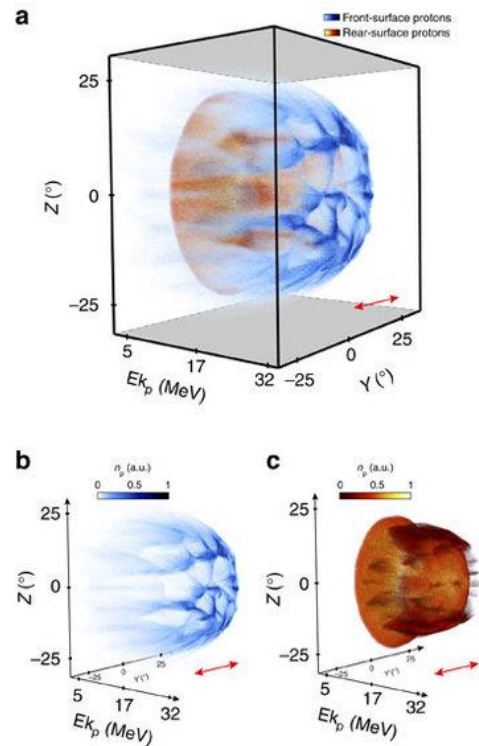


Figure 2. (a) Energy-resolved two-dimensional proton density distribution at $X=8.5 \mu\text{m}$. The blue and red distributions correspond to protons originating at the target front and rear surfaces, respectively. The same two distributions are plotted separately in (b) and (c) for clarity.

Additional numerical work was conducted through three-dimensional hybrid PIC simulations, in order to investigate the sensitivity of annular fast electron transport patterns in silicon to the properties of the drive laser pulse. It was found that the annular transport, induced by self-generated resistive magnetic fields, was particularly sensitive to the peak laser pulse intensity. The radius of the annular fast electron distribution can be varied by changing the drive laser pulse properties, and in particular the focal spot size. An ability to optically 'tune' the properties of an annular fast electron transport pattern could have important implications for the development of advanced ignition schemes and for tailoring the properties of beams of laser-accelerated ions. This was published in *Plasma Physics and Controlled Fusion* [2].

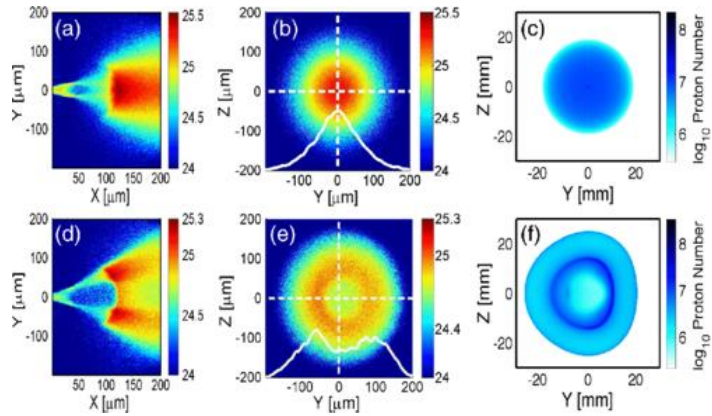


Figure 3. 3D hybrid-PIC simulation results showing \log_{10} fast electron density maps (m^{-3}), in the [X-Y] mid-plane and rear surface [Y-Z] plane, 1.4 ps and 1.6 ps after laser irradiation respectively, for the case of: (a) and (b) initially unheated Si (i.e., ordered lattice); and (d) and (e) initial heating and disorder gradients at 45° ; all for peak intensity equal to $7 \times 10^{19} \text{ Wcm}^{-2}$. (c) and (f) are the corresponding modelled proton-spatial intensity maps [1].

The influence of low temperature (eV to tens-of-eV) electrical resistivity on the onset of the filamentation instability in fast-electron transport was also investigated in targets comprising of layers of ordered (diamond) and disordered (vitreous) carbon. It is shown experimentally and numerically that the thickness of the disordered carbon layer influences the degree of filamentation of the fast-electron beam. Strong filamentation is produced if the thickness is of the order of $60 \mu\text{m}$ or greater, for an electron distribution driven by a sub-picosecond, mid- 10^{20} Wcm^{-2} laser pulse. It is shown that the position of the vitreous carbon layer relative to the fast-electron source (where the beam current density and background temperature are highest) does not have a strong effect because the resistive filamentation growth rate is high in disordered carbon over a wide range of temperatures up to the Spitzer regime, as can be seen in figure 4. This work was published in *Plasma Physics and Controlled Fusion* [3].

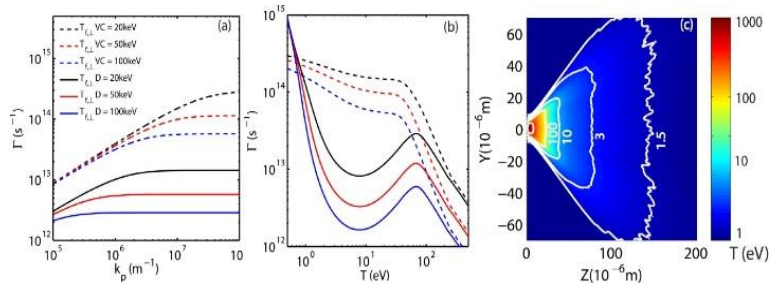


Figure 4. Resistive instability growth rate as a function of (a) wave number and (b) temperature, for vitreous carbon (VC) and diamond (D), at three example beam transverse temperatures (given). The dashed lines correspond to VC and the solid lines are for D; (c) Example 2D temperature map (eV) in the Y-Z mid-plane at 1.2 ps. Contours are drawn for isothermals corresponding to 1.5, 3, 10 and 100 eV [3].

Additional investigations into the role of low-temperature electrical resistivity in defining the transport properties of mega-Ampere currents of fast (MeV) electrons in solids were also undertaken using 3D hybrid PIC simulations. By considering resistivity profiles intermediate to the ordered (lattice) and disordered forms of two example materials, lithium and silicon, it is shown that both the magnitude of the resistivity and the shape of the resistivity-temperature profile at low temperatures strongly affect the self-generated resistive magnetic fields and the onset of resistive instabilities, and thus the overall

fast electron beam transport pattern. The scaling of these effects to the giga-Ampere electron currents is also explored. The fast electron beam transport pattern is effectively mapped into the beam of accelerated protons via spatial-intensity modulations in the sheath field. This work was published in *Plasma Physics and Controlled Fusion* [4].

Another important aspect of laser energy absorption into fast electrons (and thus ions) during the interaction of an ultra-intense (10^{20} Wcm $^{-2}$), picosecond laser pulse with a solid is also investigated, experimentally and numerically, as a function of the plasma density scale length at the irradiated surface. It is shown that there is an optimum density gradient for efficient energy coupling to electrons and that this arises due to strong self-focusing and channeling driving energy absorption over an extended length in the preformed plasma. At longer density gradients the laser filaments, resulting in significantly lower overall energy coupling. As the scale length is further increased, a transition to a second laser energy absorption process is observed experimentally via multiple diagnostics. The results demonstrate that it is possible to significantly enhance laser energy absorption and coupling to fast electrons and ions by dynamically controlling the plasma density gradient. This work was published in *Plasma Physics and Controlled Fusion* [6].

4.3 Ion acceleration from ultrathin targets

Ion acceleration driven by the interaction of an ultraintense (2×10^{20} W cm $^{-2}$) laser pulse with an ultrathin (40 nm) foil target was experimentally and numerically investigated. Protons accelerated by sheath fields and via laser radiation pressure are angularly separated and identified based on their directionality and signature features (e.g. transverse instabilities) in the measured spatial-intensity distribution. A low divergence, high energy proton component was detected when the heated target electrons expand and the target becomes relativistically transparent during the interaction.

2D and 3D particle-in-cell simulations indicated, for the first time, that under these conditions a plasma jet is formed at the target rear, supported by a self-generated azimuthal magnetic field, which extends into the expanded layer of sheath-accelerated protons. Electrons trapped within this jet are directly accelerated to super-thermal energies by the portion of the laser pulse transmitted through the target, as demonstrated in figure 5. The resulting streaming of the electrons into the ion layers enhances the energy of protons in the vicinity of the jet. Through the addition of a controlled prepulse, the maximum energy of these protons is demonstrated experimentally and numerically to be sensitive to the picosecond rising edge profile of the laser pulse. This work was published in *New Journal of Physics* [7]

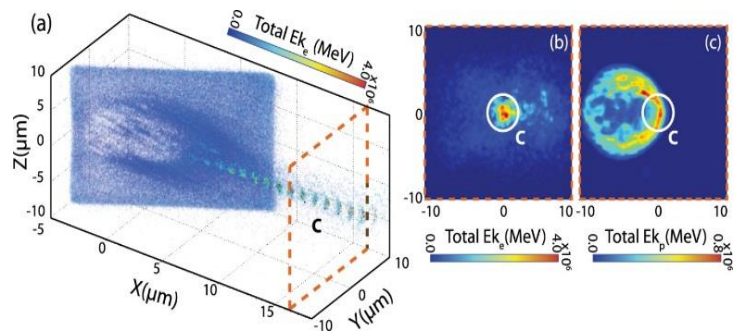


Figure 5. 3D PIC results showing (a) an example 3D plot of the total electron energy showing the formation of an electron jet, which couples energy into ions (b) electron and (c) proton energies in the Y–Z plane at $X = 16 \mu\text{m}$. At this relatively small distance from the target the jet is on-axis and overlaps with one side of the expanding proton ring distribution [7].

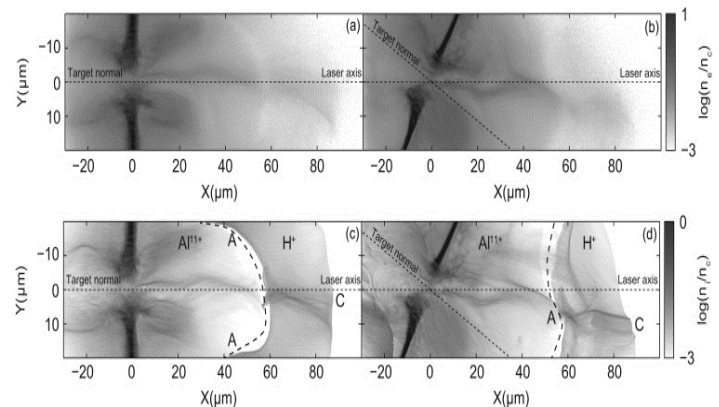


Figure 6. Top row: 2D PIC results showing electron density for the target initialised at (a) 0° and (b) 30° incident angle to the laser. Bottom row: density of the Al^{11+} and H^+ ions initialised at (c) 0° and (d) 30° incident angle to the laser. All plots are shown at an example time of 0.3 ps after the peak of the laser pulse has reached the target surface. The laser pulse is incident from the left along the $Y=0$ axis. The dotted lines mark the laser and target normal axes [5].

The effects of this electron jet, formed when the target becomes relativistically transparent, and its effects on other ion acceleration mechanisms were further investigated. By spatially resolving the laser-accelerated proton beam at near-normal laser incidence and at an incidence angle of 30° , we identify characteristic features both experimentally and in particle-in-cell simulations which are consistent with the onset of three distinct ion acceleration mechanisms: (1) sheath acceleration; (2) radiation pressure acceleration; and (3) transparency-enhanced acceleration. The latter mechanism occurs late in the interaction and is mediated by the formation of a plasma jet extending into the expanding ion population. The effect of laser incident angle on the plasma jet is explored with example numerical results shown in figure 6. This work was published in *Nuclear Instruments and Methods A* [5].

It was also found that due to the complex electron dynamics and multiple ion acceleration mechanisms that can take place in the interaction of an ultra-intense laser pulse with a thin foil, it is possible for multiple charged particle populations to overlap in space with varying momentum distributions. In certain scenarios this can drive streaming instabilities such as the relativistic Buneman instability and the ion-ion acoustic instability. The potential for such instabilities to occur are demonstrated using particle-in-cell simulations. It is shown that if a population of ions can be accelerated such that it can propagate through other slowly expanding ion populations, energy exchange can occur via the ion-ion acoustic instability. This work was published in *Plasma Physics and Controlled Fusion* [9].

As the various ion acceleration mechanisms occur during the irradiation of an ultrathin foil with intense laser pulses, the dominant mechanism can also change over the course of the interaction. A systematic measurement of the spatial-intensity distribution of the beam of energetic protons was used to investigate the transition from radiation pressure acceleration to transparency-driven processes. It is shown numerically that radiation pressure drives an increased expansion of the target ions within the spatial extent of the laser focal spot, which induces a radial deflection of relatively low energy sheath-accelerated protons to form an annular distribution. Through variation of the target foil thickness, the opening angle of the ring is shown to be correlated to the point in time that relativistic induced transparency occurs during the interaction and is maximized when it occurs at the peak of the laser intensity profile, as shown in figure 7. Corresponding experimental measurements of the ring size variation with target thickness exhibit the same trends and provide insight into the intra-pulse laser-plasma evolution. This work was published in *Physics of Plasmas* [10].

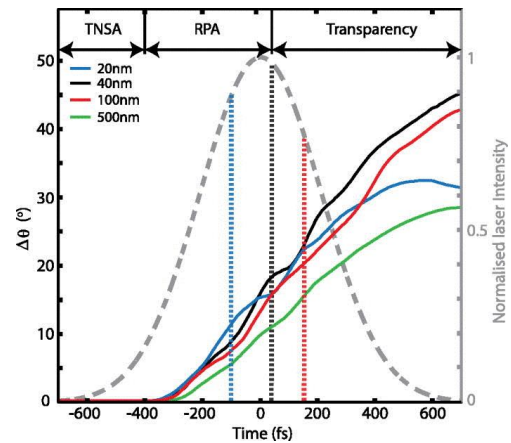


Figure 7. Simulation results showing the temporal behaviour of the average ring divergence angle for given target thicknesses. The temporal profile of the laser intensity is also shown with dashed vertical lines added to indicate the onset of transparency for the corresponding target thickness. The dominant intra-pulse acceleration mechanisms changes over the duration of the laser pulse (labelled at the top of the figure for the 40 nm case) [10].

5. CONCLUSIONS

This research undertaken in the course of this grant has resulted in the advancement of the physics underpinning the acceleration of ions from intense laser interactions with solid targets. Many underlying aspects affecting the various ion acceleration mechanisms have been elucidated. By investigating the effects of fast-electron transport through solid density targets, the effects of lattice melt and resistivity have been demonstrated to play an important role in the formation of the sheath fields at the rear surface of the target. This can lead to unstable behaviour that can break-up the fast-electron beam, impacting upon the spatial structure of the accelerated ion beam. Whilst this is mostly prevalent in micron-scale targets, it is an important aspect of laser-matter interactions and may still play a reduced role in the initial TNSA mechanisms seen in sub-micron targets.

It has been demonstrated through this work that multiple ion acceleration mechanisms occur over the course of the laser pulse interaction with sub-micron-thick targets. We have developed new techniques,

based on measuring correlations of the low-energy annular profile of the accelerated proton beams, to experimentally determine the intra-pulse transition between these mechanisms. Importantly, we have found that whilst the thin targets that undergo relativistic transparency can be detrimental to the RPA mechanism, additional energy can be coupled into a localised region of the proton beam via a directly accelerated electron jet. The directionality of this jet was found to vary based on the angle of incidence of the laser.

Finally, and perhaps most significantly, during the course of this work we have discovered that as the target becomes relativistically transparent in a localised region of the target, forming what has been termed a 'relativistic plasma aperture', the propagating laser pulse diffracts as it passes through. As the laser is still of high intensity, the near-field diffraction pattern directly affects the electron structure at the rear of the target. This can directly map into the accelerated proton beam and therefore can provide a purely optical method of controlling the resulting accelerated spatial structures. We demonstrated that by varying the polarisation of the incoming laser pulse, the resultant diffraction pattern is changed in a predictable way and can therefore be used to manipulate the ion and electron beam spatial profile. All of these results have greatly enhanced the understanding of the physics of intense laser-dense matter interactions underpinning the development of laser-driven ion sources. These results will provide a foundation to build towards more compact laser-driven ion sources for wide ranging applications.

6. PUBLICATIONS ARISING FROM THE GRANT

1. Gonzalez-Izquierdo, B., et al. "Optically controlled dense current structures driven by relativistic plasma aperture-induced diffraction." *Nature Physics* **12**, 505512 (2016)
2. Gonzalez-Izquierdo, B., et al. "Towards optical polarization control of laser-driven proton acceleration in foils undergoing relativistic transparency." *Nature Communications* **7** (2016): 12891
3. Gray, R. J., et al. "Azimuthal asymmetry in collective electron dynamics in relativistically transparent laser-foil interactions." *New Journal of Physics* **16**, 093027 (2014)
4. Gonzalez-Izquierdo, B., et al. "Influence of laser polarization on collective electron dynamics in ultraintense laser-foil interactions." *High Power Laser Science and Engineering* **4** (2016)
5. MacLellan, D. A., et al. "Tunable mega-ampere electron current propagation in solids by dynamic control of lattice melt." *Physical review letters* **113**, 185001 (2014)
6. MacLellan, D. A., et al. "Influence of laser-drive parameters on annular fast electron transport in silicon." *Plasma Physics and Controlled Fusion* **56**, 084002 (2014)
7. Dance, R. J., et al. "Role of lattice structure and low temperature resistivity in fast-electron-beam filamentation in carbon." *Plasma Physics and Controlled Fusion* **58**, 014027 (2015)
8. McKenna, P., et al. "Influence of low-temperature resistivity on fast electron transport in solids: scaling to fast ignition electron beam parameters." *Plasma Physics and Controlled Fusion* **57**, 064001 (2015)
9. Gray, R. J., et al. "Laser pulse propagation and enhanced energy coupling to fast electrons in dense plasma gradients." *New Journal of Physics* **16**, 113075 (2014)
10. Powell, H. W., et al. "Proton acceleration enhanced by a plasma jet in expanding foils undergoing relativistic transparency." *New Journal of Physics* **17**, 103033 (2015)
11. King, M., et al. "Ion acceleration and plasma jet formation in ultra-thin foils undergoing expansion and relativistic transparency." *Nuclear Instruments and Methods in Physics Research Section A: Accelerators, Spectrometers, Detectors and Associated Equipment* **829**, 163166 (2016)
12. Padda, H., et al. "Intra-pulse transition between ion acceleration mechanisms in intense laser-foil interactions." *Physics of Plasmas* **23**, 063116 (2016)
13. King, M., et al. "Energy exchange via multi-species streaming in laser-driven ion acceleration." *Plasma Physics and Controlled Fusion* **59**, 014003 (2016)

7. ADDITIONAL REFERENCES

14. Wilks, S. C., et al. "Energetic proton generation in ultra-intense laser–solid interactions." *Physics of plasmas* **8**, 542549 (2001):
15. Esirkepov, T., et al. "Highly efficient relativistic-ion generation in the laser-piston regime." *Physical review letters* **92**, 175003 (2004)
16. Macchi, Andrea, et al. "Radiation pressure acceleration of ultrathin foils." *New Journal of Physics* **12**, 045013 (2010)
17. Kar, S., et al. "Ion acceleration in multispecies targets driven by intense laser radiation pressure." *Physical Review Letters* **109**, 185006 (2012)
18. Palmer, C. A. J., et al. "Rayleigh-taylor instability of an ultrathin foil accelerated by the radiation pressure of an intense laser." *Physical review letters* **108**, 225002 (2012)
19. Vshivkov, V. A., et al. "Nonlinear electrodynamics of the interaction of ultra-intense laser pulses with a thin foil." *Physics of Plasmas* **5**, 2727-2741 (1998)
20. Yin, L., et al. "GeV laser ion acceleration from ultrathin targets: The laser break-out afterburner." *Laser and Particle Beams* **24**, 291298 (2006)
21. Jung, D., et al. "Beam profiles of proton and carbon ions in the relativistic transparency regime." *New Journal of Physics* **15**, 123035 (2013)